Relativistic Magnetohydrodynamics
An introduction and selected simulation results

Rony Keppens

including work with Z. Meliani, O. Porth, S. Komissarov, et al.

Centre for mathematical Plasma-Astrophysics
Department of Mathematics, KU Leuven

Outline

- Special relativistic MHD introduction
  - ⇒ **SRMHD** equations
  - ⇒ linear waves in homogeneous media
  - ⇒ RMHD shock relations
- **Relativistic MHD simulations**: `MPI-AMRVAC`
  - ⇒ relativistic (M)HD two-component jet simulations
  - ⇒ helically magnetized, relativistic jets
  - ⇒ Crab nebula simulations
- Outlook

- lecture material from modern (2004 & 2010) textbooks
  - $\Rightarrow$ **Goedbloed** et al., Cambridge University Press
  - $\Rightarrow$ chapter 21 on relativistic MHD ...

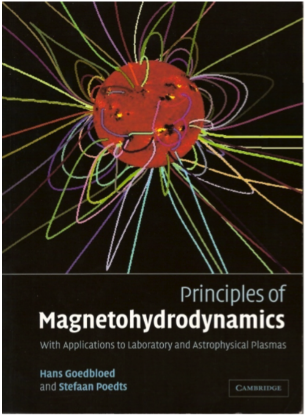

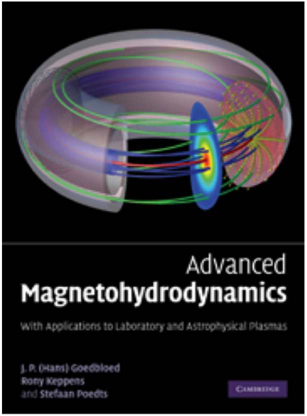

Special Relativity I

- 4D flat space-time, with c as maximal propagation speed
  - $\Rightarrow$ four-vector $\mathbf{X} = (ct, \mathbf{x})^T$ squared length invariant

$$\mathbf{X} \cdot \mathbf{X} = -c^2 t^2 + x_1^2 + x_2^2 + x_3^2$$

  - $\Rightarrow$ Minkowski metric $g_{\alpha\beta} = g^{\alpha\beta} = \mathrm{diag}\,(-1, 1, 1, 1)$
  - $\Rightarrow$ contra- & covariant components $X^\alpha = g^{\alpha\beta} X_\beta$: only reverse $X^0 = -X_0$
- particle wordline: ideal clock for proper time τ

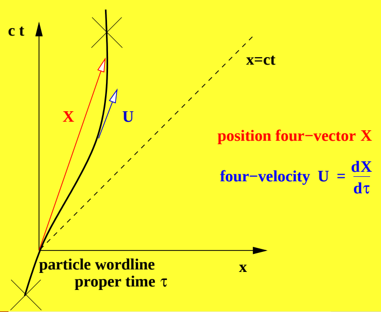

Special Relativity II

- tangent fourvector to worldline

  $\Rightarrow$ four-velocity $\mathbf{U} = \mathbf{dX}/d\tau$, components

$$U^\alpha = \left(c \underbrace{\frac{dt}{d\tau}}_{\text{dilation}}, \underbrace{\frac{dx_i}{dt}}_{v_i} \frac{dt}{d\tau} \right) = (c\Gamma, \Gamma\mathbf{v})^T$$

  $\Rightarrow$ spatial three-velocity $\mathbf{v}$ in chosen Lorentzian lab frame

  $\Rightarrow$ Lorentz factor $\Gamma = \frac{1}{\sqrt{1-v^2/c^2}}$

Special Relativity III

- inertial frames Lorentz transform $\mathbf{X}' = L_{\alpha}^{\alpha'}\mathbf{X}$

  $\Rightarrow$ lost simultaneity, length contracts, time dilates
- proper density: $\rho = m_0 n_0$ with n_0 rest frame number density

  $\Rightarrow$ lab 'density' $D = \Gamma\rho$: volume change by length contraction
- Particle conservation is $\partial_\alpha\left(\rho U^\alpha\right) = 0$ or

$$\frac{\partial D}{\partial t} + \nabla\cdot(D\mathbf{v}) = 0$$

- stress-energy tensor:

$$\begin{pmatrix} T^{00} & T^{0i} \\ T^{i0} & T^{ij} \end{pmatrix} = \begin{pmatrix} \text{energy density} & \text{energy flux} \\ \text{momentum flux} & \text{stresses} \end{pmatrix}$$

- gas stress-energy contribution from expression in rest frame:

$$\begin{pmatrix} \underbrace{\rho c^2 + \rho\epsilon}_{\text{rest mass + internal energy}} & \mathbf{0} \\ \mathbf{0} & \underbrace{p\mathbf{I}}_{\text{isotropic pressure}} \end{pmatrix}$$

$\Rightarrow$ to lab frame by inverse Lorentz $T^{\alpha\beta} = L^{-1,\alpha}_{\alpha'} L^{-1,\beta}_{\beta'} T^{\alpha'\beta'}$

$$\begin{pmatrix} T^{00} & T^{0i} \\ T^{i0} & T^{ij} \end{pmatrix} = \begin{pmatrix} \tau_{\mathrm{g}} + Dc^2 & \frac{\mathbf{S}_{\mathrm{g}}}{c} \\ \frac{\mathbf{S}_{\mathrm{g}}}{c} & \frac{\mathbf{S}_{\mathrm{g}}\mathbf{v}}{c^2} + p\mathbf{I} \end{pmatrix}$$

$\Rightarrow$ $\mathbf{S}_{\mathrm{g}} = (\rho c^2 + \rho\epsilon + p)\Gamma^2\mathbf{v}$ and $\tau_{\mathrm{g}} + Dc^2 = (\rho c^2 + \rho\epsilon + p)\Gamma^2 - p$

Special Relativity V

- when also allowing for electromagnetic fields: EM stress-energy

$$T_{\rm em}^{\alpha\beta} = \begin{pmatrix} \underbrace{\frac{B^2}{2\mu_0} + \epsilon_0 \frac{E^2}{2}}_{\text{EM energy density}} & \frac{\mathbf{S}_{\rm em}}{c} \\ \frac{\mathbf{S}_{\rm em}}{c} & \underbrace{\left(\frac{B^2}{2\mu_0} + \epsilon_0 \frac{E^2}{2}\right)\mathbf{I} - \epsilon_0 \mathbf{EE} - \frac{\mathbf{BB}}{\mu_0}}_{\text{Maxwell stress tensor}} \end{pmatrix}$$

$\Rightarrow$ EM energy flux is Poynting flux $\mathbf{S}_{\rm em} = \frac{\mathbf{E}\times\mathbf{B}}{\mu_0}$

$\Rightarrow$ use $\mathbf{E} = -\mathbf{v} \times \mathbf{B}$: perfect conductivity

Special Relativity VI

- energy-momentum conservation

$$\partial_\beta \left(T^{\alpha\beta} + T^{\alpha\beta}_{\mathrm{em}} \right) = 0$$

- introduce energy density minus rest mass and total energy flux

$$\begin{aligned} \tau &= \tau_{\mathrm{g}} + \frac{B^2}{2\mu_0} + \epsilon_0 \frac{B^2 v^2 - (\mathbf{v}\cdot\mathbf{B})^2}{2} \\ \mathbf{S}_{\mathrm{tot}} &= \mathbf{S}_{\mathrm{g}} + \mathbf{S}_{\mathrm{em}} \end{aligned}$$

$\Rightarrow$ temporal part gives

$$\frac{\partial \tau}{\partial t} + \nabla \cdot \left((\tau + p_{\mathrm{tot}})\mathbf{v} - (\mathbf{v}\cdot\mathbf{B})\frac{\mathbf{B}}{\mu_0} \right) = 0$$

$\Rightarrow$ spatial part:

$$\frac{\partial \mathbf{S}_{\mathrm{tot}}}{\partial t} + \nabla \cdot \left(\mathbf{S}_{\mathrm{tot}}\mathbf{v} + p_{\mathrm{tot}} c^2 \mathbf{I} - \frac{c^2}{\mu_0}\frac{\mathbf{B}\mathbf{B}}{\Gamma^2} - \frac{1}{\mu_0}(\mathbf{v}\cdot\mathbf{B})\mathbf{v}\mathbf{B} \right) = \mathbf{0}$$

Special Relativity VII

- total pressure $p_{\rm tot} = p + \frac{(\mathbf{v}\cdot\mathbf{B})^2}{2c^2} + \frac{B^2}{2\Gamma^2}$
- close system with homogeneous Maxwell equations:

$$\boxed{\nabla \cdot \mathbf{B} = 0}$$

$$\boxed{\frac{\partial \mathbf{B}}{\partial t} - \nabla \times (\mathbf{v} \times \mathbf{B}) = \mathbf{0}}$$

$\Rightarrow$ together with equation of state, e.g. polytropic relation

$$\rho\epsilon = \frac{p}{\gamma - 1}$$

$\Rightarrow$ enters specific enthalpy h where $\rho h = \rho c^2 + \rho\epsilon + p$

- **Equation of state in relativistic MHD**
  - $\Rightarrow$ specific internal energy $\epsilon = p/(\gamma - 1)\rho$
  - $\Rightarrow$ assumes constant polytropic index γ
- **Relativistically correct ideal gas: effective $\hat{\gamma}(T)$**
  - $\Rightarrow$ compare Synge with Mathews proxy (no Bessel functions)

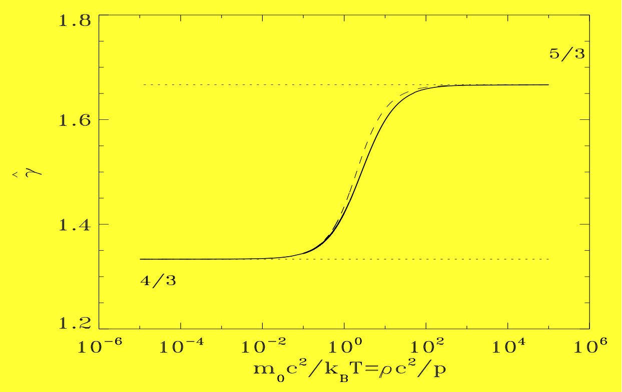

- **special relativistic magnetofluids** $\rightarrow$ flat Minkowski space-time; particle, tensorial energy-momentum conservation, full Maxwell
- **ideal magnetohydrodynamic: vanishing electric field in comoving frame**

$$\mathbf{E} = -\mathbf{v} \times \mathbf{B}$$

$\Rightarrow$ fix Lorentz frame, use $1+3$ split (time/space), obtain

$$\partial_t \mathbf{U} + \partial_i \mathbf{F}^i = 0$$

$\Rightarrow$ conserved variables $\mathbf{U} = (D, \mathbf{S}_{\mathrm{tot}}, \tau, \mathbf{B})$

$\Rightarrow$ primitives $(\rho, \mathbf{v}, p, \mathbf{B})$

Newtonian limit: Ideal MHD and conservation laws

- $\Gamma \to 1$: **conservation laws** for density ρ, momentum density $\mathbf{m} = \rho \mathbf{v}$, $\mathcal{H}$ and $\mathbf{B}$

$$\frac{\partial \rho}{\partial t} + \nabla \cdot (\mathbf{v}\rho) = 0$$

- $D \to \rho$ and $\mathbf{S}_{\mathrm{tot}} \to c^2 \rho \mathbf{v}$ and $p_{tot} \equiv$ thermal + magnetic pressure

Newtonian limit: Ideal MHD and conservation laws

- $\Gamma \to 1$: **conservation laws** for density ρ, momentum density $\mathbf{m} = \rho\mathbf{v}$, $\mathcal{H}$ and $\mathbf{B}$

$$\frac{\partial \mathbf{m}}{\partial t} + \nabla \cdot (\mathbf{v}\rho\mathbf{v} - \mathbf{B}\mathbf{B}) + \nabla p_{tot} \quad = \quad \mathbf{0}$$

- $D \to \rho$ and $\mathbf{S}_{\rm tot} \to c^2\rho\mathbf{v}$ and $p_{tot} \equiv$ thermal + magnetic pressure

Newtonian limit: Ideal MHD and conservation laws

- $\Gamma \to 1$: **conservation laws** for density ρ, momentum density $\mathbf{m} = \rho\mathbf{v}$, $\mathcal{H}$ and $\mathbf{B}$

$$\frac{\partial \mathcal{H}}{\partial t} + \nabla \cdot (\mathbf{v}\mathcal{H} + \mathbf{v}p_{tot} - \mathbf{BB}\cdot\mathbf{v}) = 0$$

- total energy density $\tau \to \mathcal{H}$ has 3 contributions

$$\mathcal{H} = \underbrace{\rho\epsilon}_{\text{internal}} + \underbrace{\frac{\rho v^2}{2}}_{\text{kinetic}} + \underbrace{\frac{1}{2}B^2}_{\text{magnetic}}$$

Newtonian limit: Ideal MHD and conservation laws

- $\Gamma \to 1$: **conservation laws** for density ρ, momentum density $\mathbf{m} = \rho\mathbf{v}$, $\mathcal{H}$ and $\mathbf{B}$

$$\frac{\partial \mathbf{B}}{\partial t} + \nabla \cdot (\mathbf{vB} - \mathbf{Bv}) = \mathbf{0}$$

- idem in relativistic/Newtonian setting

Newtonian intermezzo: wave diagrams

- **linearize (ideal) MHD equations about uniform, static state, uniform field $\mathbf{B}_0$**

  $\Rightarrow$ Lagrangian displacement ξ, normal mode analysis $e^{-\mathrm{i}\omega t}$

  $\Rightarrow$ algebraic eigenvalue problem

  $\Rightarrow$ analytic expressions for dispersion relation $\omega^2(\mathbf{k})$, when perturbations assume plane wave form

$$\hat{\xi}(\mathbf{k};\omega)\exp\mathrm{i}(\mathbf{k}\cdot\mathbf{r}-\omega t)$$

  $\Rightarrow$ Alfvén modes then e.g. $\omega_A^2 = (\mathbf{k}\cdot\mathbf{B}_0)^2/\mu_0\rho_0$

Newtonian intermezzo: wave diagrams

- **linearize (ideal) MHD equations about uniform, static state, uniform field $\mathbf{B}_0$**

  $\Rightarrow$ dispersion diagram $\omega^2 = \omega^2(k_x)$ for k_y and $k_z = k_\parallel$ fixed

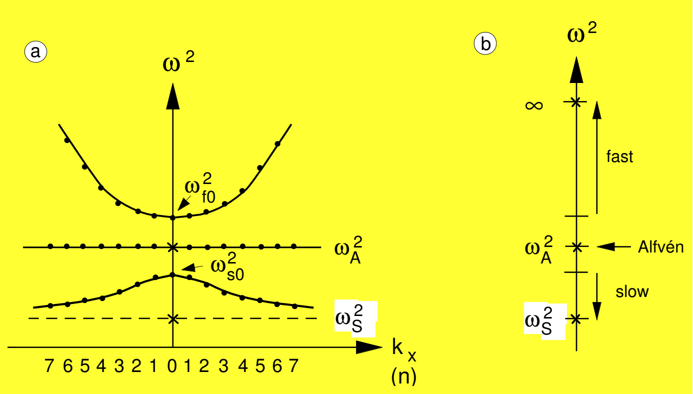

- continuous curves to quantized modes: $k_x = n\pi/a$ if $x \in [0, a]$

- phase diagram: endpoint of **k** vector as angle between **k** and $\mathbf{B}_0$ varies: for Alfvén yields two spheres left/right of origin ($\mathbf{b} = \mathbf{B}_0/\sqrt{\mu_0\rho_0}$)

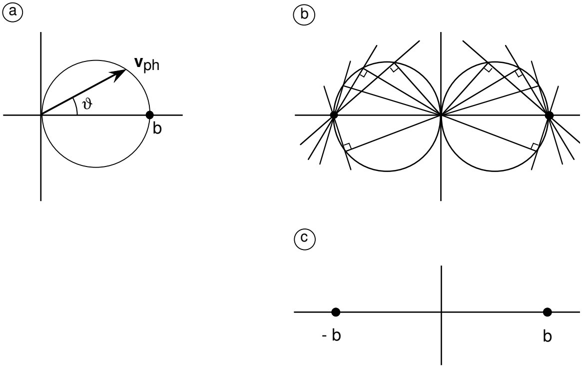

(a) Phase diagram for Alfvén waves is circle
⇒(b) wavefronts pass through **points** $\pm b$
⇒(c) those points are the group diagram.

Phase and group diagrams

Friedrichs diagrams (schematic)

parameter $c/b = \frac{1}{2}\gamma\beta\,,\ \beta \equiv 2p/B^2$

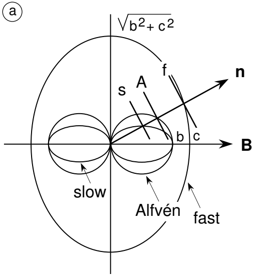

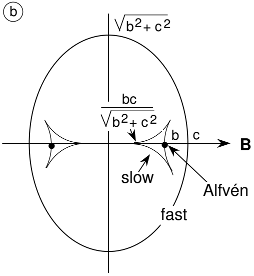

Phase diagram
(plane waves)

Group diagram
(point disturbances)

MHD waves

- 7 wavespeeds *entropy,* $\pm$ *slow,* $\pm$ *Alfvén,* $\pm$ *fast* [anisotropic!]
  - $\Rightarrow$ speeds v, $v \pm c_s$, $v \pm b$, $v \pm c_f$
  - $\Rightarrow$ **7 characteristic speeds of the hyperbolic PDE system**
- **MHD waves in uniform medium**

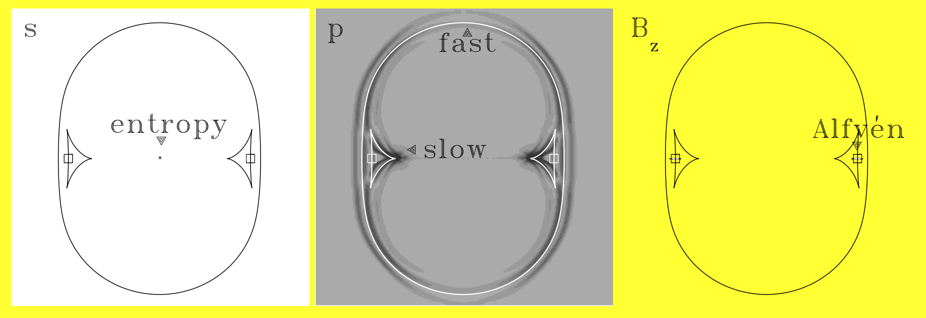

Special Relativistic HD

- **relativistic hydro in $3+1$ form** reads:

$$
\begin{aligned}
\frac{\partial S}{\partial t} &+ \mathbf{v}\cdot\nabla S = 0\,, \\
\frac{\partial \rho}{\partial t} &+ \mathbf{v}\cdot\nabla\rho + \frac{\rho h}{u}\nabla\cdot\mathbf{v} \\
&- \frac{1}{u\Gamma^2}\mathbf{v}\cdot\nabla\left(S\rho^\gamma\right) = 0\,, \\
\frac{\partial \mathbf{v}}{\partial t} &+ \left(\mathbf{v}\cdot\nabla\right)\mathbf{v} + \frac{c^2}{\rho h\Gamma^2}\nabla\left(S\rho^\gamma\right) \\
&- \mathbf{v}\left(\nabla\cdot\mathbf{v}\right)\left[1-\frac{yc^2}{u}\right] - \mathbf{v}\frac{yc^2}{u\rho h\Gamma^2}\mathbf{v}\cdot\nabla\left(S\rho^\gamma\right) = 0\,.
\end{aligned}
$$

$\Rightarrow$ using entropy $S = p\rho^{-\gamma}$, rest frame density ρ, 3-velocity $\mathbf{v}$

Linear waves in RHD I

- linearize about **static $\mathbf{v} = 0$, uniform gas (constant S, ρ)**

  $\Rightarrow$ assume plane wave variation of linear quantities $S_1, \rho_1, \mathbf{v}_1$

$$\exp(-i\omega t + i\mathbf{k} \cdot \mathbf{x})$$

- obtain **in chosen (rest) Lorentz frame**

$$\begin{aligned}
\omega S_1 &= 0 \,, \\
\omega \rho_1 &= \rho \mathbf{k} \cdot \mathbf{v}_1 \,, \\
\omega \mathbf{v}_1 &= \frac{c^2}{\rho h} \mathbf{k} \left(S \gamma \rho^{\gamma-1} \rho_1 + \rho^{\gamma} S_1 \right) \,.
\end{aligned}$$

$\Rightarrow$ five solutions, **entropy + shear waves at $\omega = 0$, two sound waves**

Linear waves in RHD II

- sound waves **dispersion relation**

$$\frac{\omega^2}{k^2 c^2} = \frac{\gamma S \rho^{\gamma-1}}{h} = \frac{\gamma p}{\rho h} = \frac{c_g^2}{c^2}$$

$\Rightarrow$ phase speed for plane wave with wavevector $\mathbf{k} = k\mathbf{n}$ from

$$\frac{\mathbf{v}_{\mathrm{ph}}}{c} = \frac{c_g}{c}\mathbf{n}$$

Linear waves in RHD III

- vary direction of wavevector over 2π, obtain phase diagram

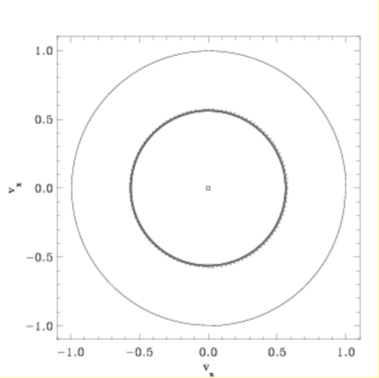

$\Rightarrow$ isotropic propagation at sound speed

$\Rightarrow$ **group** (energy propagation) and phase speed coincide

$$\frac{\mathbf{v}_{\mathrm{gr}}}{c} = \frac{\partial \omega}{\partial \mathbf{k}} = \frac{c_g}{c}\mathbf{n}$$

Linear waves in RHD IV

- in frame L' where source moves at velocity $\mathbf{v}$

  $\Rightarrow$ Lorentz transform: L' coordinates $(ct', \mathbf{x}')$ and L with $(ct, \mathbf{x})$

- **plane wave in L' with** $\exp(-i\omega' t' + i\mathbf{k}' \cdot \mathbf{x}')$ **still plane wave in L with** $\exp(-i\omega t + i\mathbf{k} \cdot \mathbf{x})$

  $\Rightarrow$ changed frequency: **relativistic Doppler effect**

  $\Rightarrow$ altered wave vector direction: **Relativistic wave aberration**

$$
\begin{aligned}
\omega &= \Gamma \left(\omega' + \mathbf{k}' \cdot \mathbf{v}\right) \ , \\
\mathbf{k} &= \mathbf{k}' + \mathbf{v} \left[\frac{\omega' \Gamma}{c^2} + \left(\mathbf{k}' \cdot \mathbf{v}\right) \frac{\Gamma - 1}{v^2} \right]
\end{aligned}
$$

Linear waves in RHD V

- phase speed relation is then

$$\frac{v'^2_{\rm ph}}{c^2} = \frac{\Gamma^2 \left(v_{\rm ph} - \mathbf{n}\cdot\mathbf{v}\right)^2}{c^2 + \Gamma^2\left(v_{\rm ph} - \mathbf{n}\cdot\mathbf{v}\right)^2 - v_{\rm ph}^2}$$

$\Rightarrow$ graphically: **phase diagram for moving source (wave aberration)**

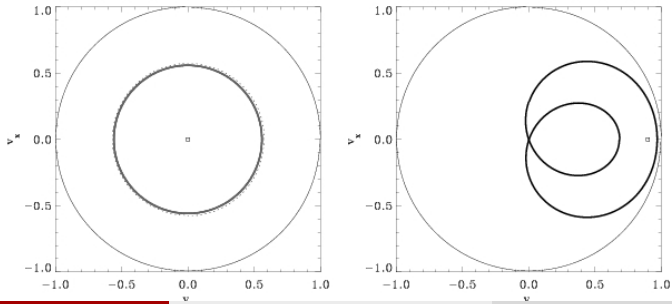

Linear waves in RHD VI

- **Group diagram** in same Lorentz frame: use **Huygens construction**

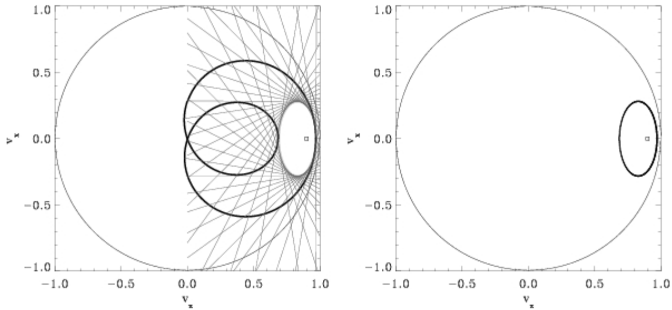

$\Rightarrow$ group diagram: **observed wavefront for moving point source**

Relativistic MHD waves I

- in MHD: anisotropic wave behavior **in rest frame**

  ⇒ phase & group (Friedrich) diagrams for slow, Alfvén, fast

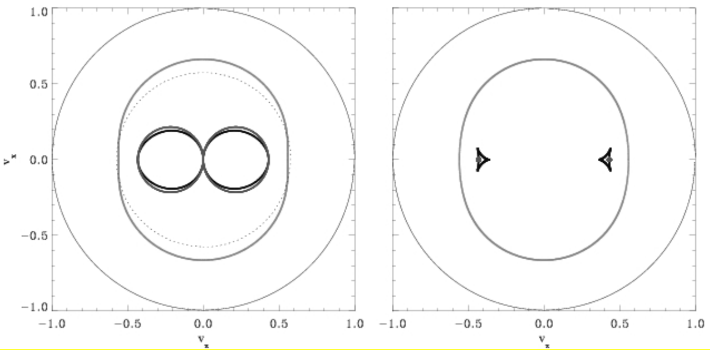

  ⇒ horizontal **B**, uniform plasma

  ⇒ δ-perturbation yields group diagram, also Huygens construction

Relativistic MHD waves II

- Alfvén waves as source moves at
  $\mathbf{v} = 0.9\,[\sin(\pi/4)\mathbf{e}_x + \cos(\pi/4)\mathbf{e}_z]$
  $\Rightarrow$ circular phase diagrams get displaced

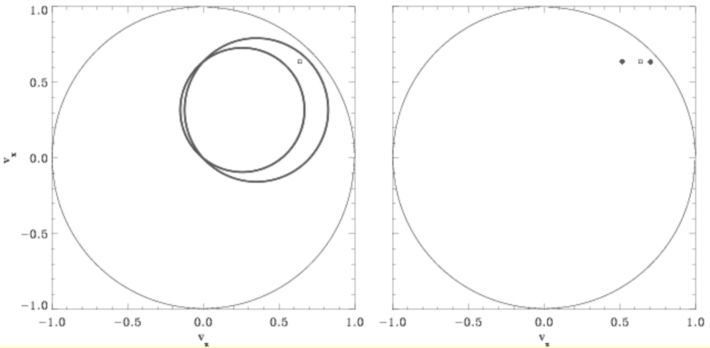

$\Rightarrow$ group diagram: **Alfvén pulse traveling along perturbed fieldline**

Relativistic MHD waves III

- Depending on uniform medium: **Alfvén & fast speeds may approach *c***

  $\Rightarrow$ phase and group diagrams for slow, Alfvén, fast modes **in rest frame**

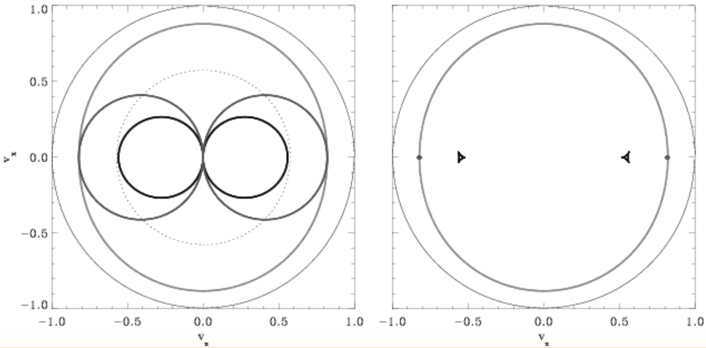

Relativistic MHD waves IV

- same case: draw **phase diagram when source moves at**

$$\mathbf{v} = 0.9\,[\sin(\pi/4)\mathbf{e}_x + \cos(\pi/4)\mathbf{e}_z]$$

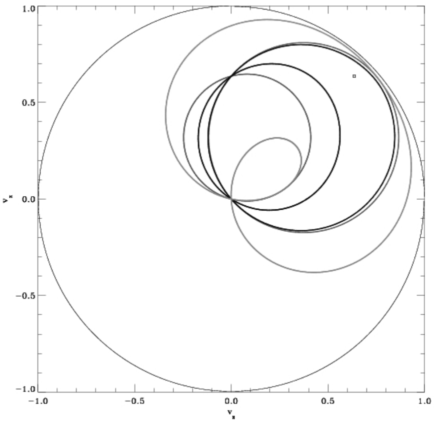

Relativistic MHD waves V

- group speed diagram then fully 3D objects, no more symmetry

  $\Rightarrow$ use **Huygens constructions: slow and fast fronts**

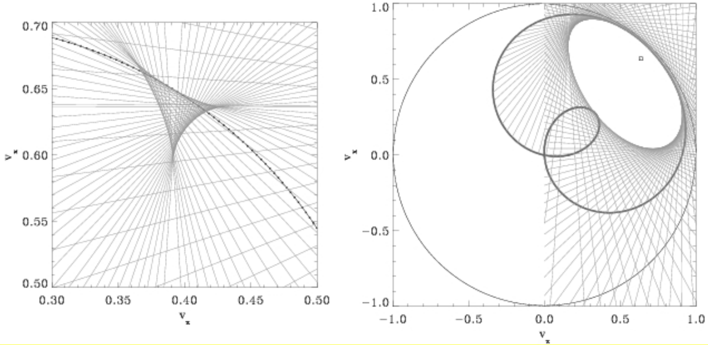

Relativistic MHD waves VI

- when speed $\mathbf{v} = 0.9c\mathbf{e}_z$ aligned with $\mathbf{B}$, still up-down symmetry
  $\Rightarrow$ from Lorentz transform get group diagram

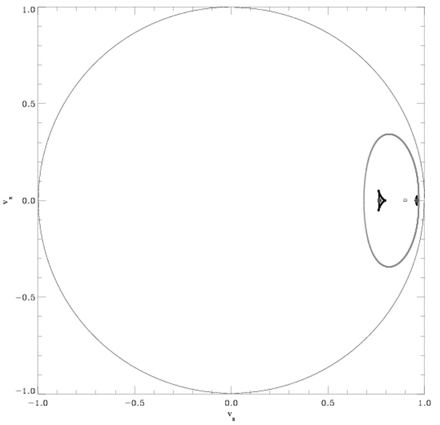

- see **Physics of Plasmas 15, 102103, 2008**

- MHD wave speed expressions: analytic expressions for entropy and Alfvén phase speeds, while fast and slow pairs from quartic polynomial (can use e.g. Laguerre iteration to locate roots)

  $\Rightarrow$ needed for solvers like TVDLF, HLL(C), … (characteristic wave speeds)

Relativistic MHD shocks

- shockfront: discontinuity across 4-manifold $\phi(ct, \mathbf{x}) = 0$

  $\Rightarrow$ normal to shockfront: space-like 4-vector $\mathbf{l}$, components $l_\alpha = \partial_\alpha \phi$

  $\Rightarrow$ Rankine-Hugoniot express conservation across manifold

$$
\begin{aligned}
[\![\rho U^\alpha]\!] l_\alpha &= 0 \\
[\![T^{\alpha\beta}]\!] l_\alpha &= 0
\end{aligned}
$$

  $\Rightarrow$ directly follow from laws $\partial_\alpha(\rho U^\alpha) = 0$ and $\partial_\alpha(T^{\alpha\beta}) = 0$

- four-vector for magnetic field (ideal MHD)

$$
b^\alpha = \left[\Gamma \frac{\mathbf{v} \cdot \mathbf{B}}{c}, \frac{\mathbf{B}}{\Gamma} + \Gamma(\mathbf{v} \cdot \mathbf{B})\mathbf{v}/c^2\right]^{\mathrm{T}}
$$

  $\Rightarrow$ induction equations yields

$$
[\![U^\alpha b^\beta - b^\alpha U^\beta]\!] l_\alpha = 0
$$

- involved relations, add complication of different reference frames

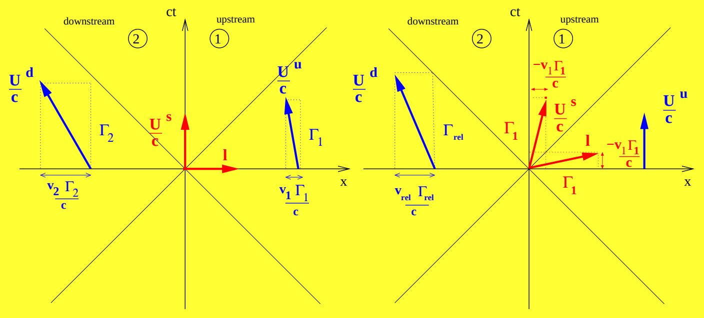

$\Rightarrow$ in SRF (left): $\mathbf{l} = (0, \mathbf{e}_x)$, with four-velocities up/downstream

$$
\begin{aligned}
\mathbf{U}^{\mathrm{u}} &= (c\Gamma_1, \Gamma_1 \mathbf{v}_1) \\
\mathbf{U}^{\mathrm{d}} &= (c\Gamma_2, \Gamma_2 \mathbf{v}_2)
\end{aligned}
$$

- many relativistic MHD shock invariants known, e.g. Lichnerowicz adiabat (like Hugoniot/Taub adiabat)

Adaptive Mesh Refinement & MPI-AMRVAC

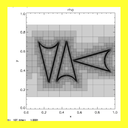

- extreme contrasts, positive p, ρ, τ, $v < 1$, $\Gamma \geq 1$, solenoidal $\mathbf{B}$

  $\Rightarrow$ stringent demands on numerics and accuracy: **AMR vital**
- **Special relativistic HD and MHD: 'modules' in MPI-AMRVAC**

  $\Rightarrow$ *CPC* **179** 2008, 617, *JCP* **226** 2007, 925, *MNRAS* **376** 2007, 1189, *JCP* **231** 2013, 718

  $\Rightarrow$ advection, hydro, MHD, relativistic (M)HD modules

  $\Rightarrow$ **different EOS implemented for relativistic modules**

  $\Rightarrow$ any-D, explicit **grid adaptive framework**

  $\Rightarrow$ **full MPI octree variant, cartesian/cylindrical/spherical**
- shock-capturing schemes (TVDLF/HLL/HLLC/Roe), 2nd to higher order reconstructions

RMHD Orszag-Tang test

- relativistic analogue of 2D MHD Orszag-Tang test
  - $\Rightarrow$ double periodic, supersonic relativistic vortex rotation
  - $\Rightarrow$ initial field configuration: double island structure

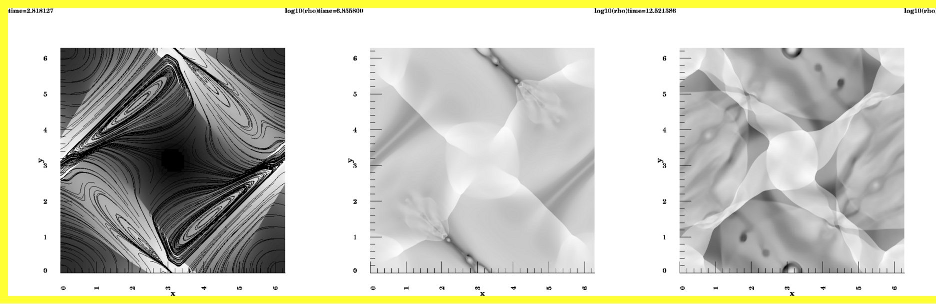

$\Rightarrow$

current sheets form, shock interactions, reconnections

- AMR vital: captures small-scale ‘reconnection’ effects

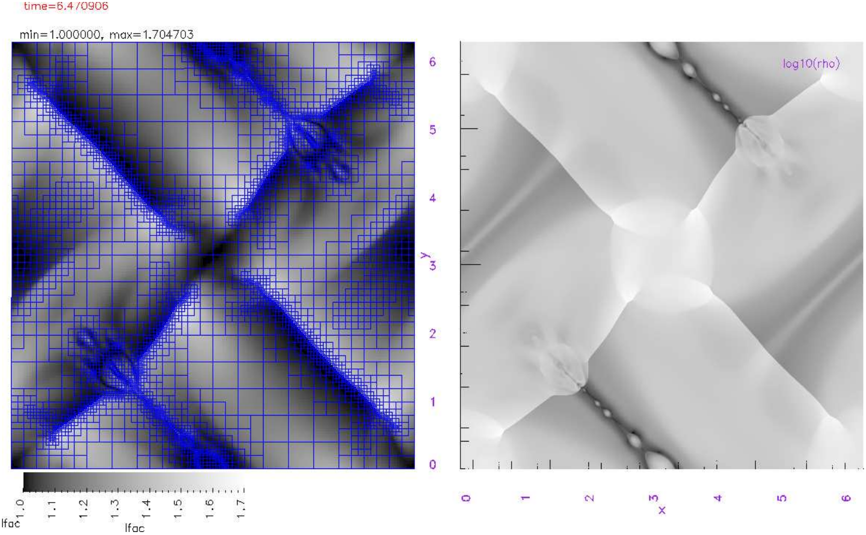

$\Rightarrow$ to revisit in true resistive RMHD!

RMHD wave test

- linear waves in homogeneous plasma with $\rho = 1 = p$

  $\Rightarrow$ uniform $\mathbf{B} = 0.3\mathbf{e}_x$, perturb with $\delta p = 0.1 = \delta v_z$

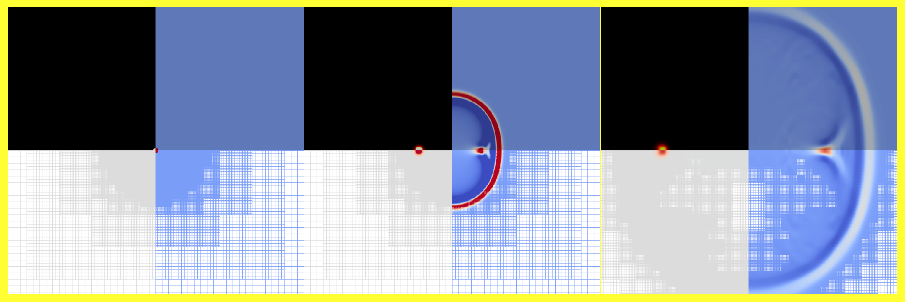

$\Rightarrow$ **triggers all 3 wave signals**, reproduces group diagram

$\Rightarrow$ note: AMR only active late: typical easy to detect shocks!

MPI-AMRVAC and HPC-Europa2

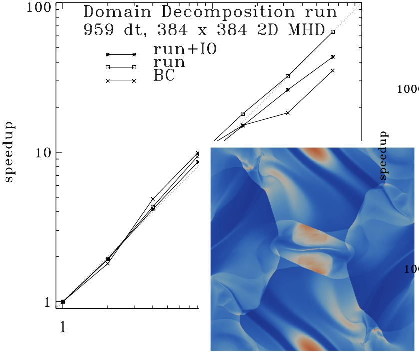

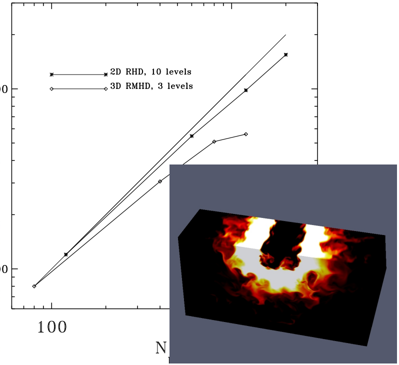

- **excellent scaling**: domain decomposition and **multi-level AMR**

  $\Rightarrow$ 2D MHD at $\simeq 400^2$, 1000 Δt in $<$ 5 seconds (include IO)

  $\Rightarrow$ **10 level AMR special relativistic HD sustained 80% efficiency on 2000 CPUs!**

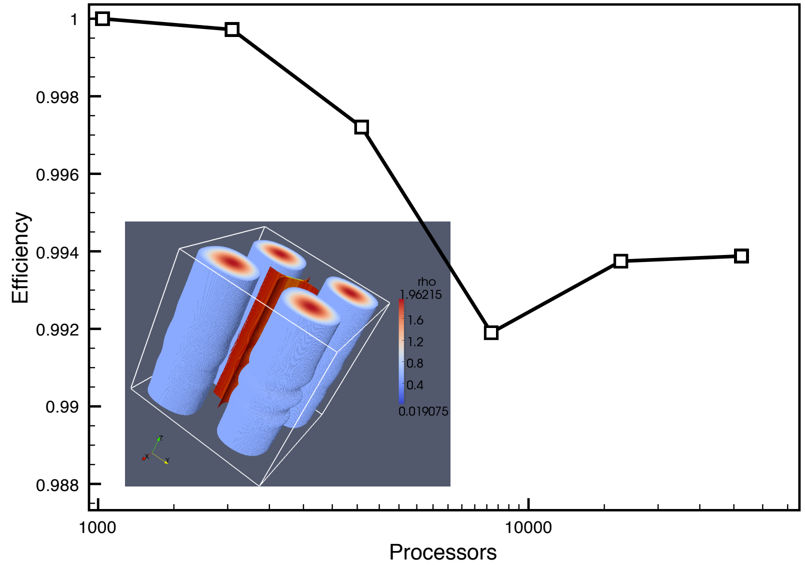

- 3D MHD weak scaling to $>$31000 CPUs (Fermi)

- conservative to primitive transformation: no longer purely algebraic as in Newtonian MHD

  $\Rightarrow$ in each grid point, local rootfinding required

  $\Rightarrow$ many equivalent formulations exist: accuracy/speed crucial in selection
- MPI-AMRVAC: use auxiliary variables $(\xi = \rho h \Gamma^2, \Gamma)$

  $\Rightarrow$ nonlinear transcendental equation solves ξ from

$$0 = \xi - p - \tau - D + B^2 - \frac{1}{2}\left[\frac{B^2}{\Gamma^2} + \frac{(\mathbf{S}_{\mathrm{tot}} \cdot \mathbf{B})^2}{\xi^2}\right]$$

Internal stratification effects and jet deceleration

- AGN jets **radial stratification: fast inner, slow outer jet**
  $\Rightarrow$ different launch mechanism $\rightarrow$ different rotation
- **outer 'disk' jet launched magnetocentrifugally**
  $\Rightarrow$ Magnetized Accretion-Ejection Structure (MAES)

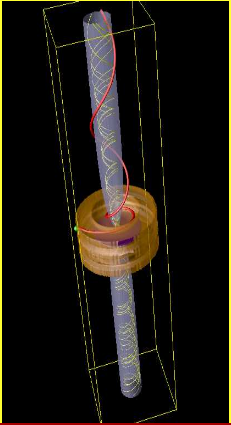

- generic mechanism for jet launch
  - $\Rightarrow$ magnetic torque brakes disk matter
  - $\Rightarrow$ magnetic torque spins up jet matter
  - $\Rightarrow$ mass source for jet: disk
  - $\Rightarrow$ **B** collimates, accelerates
  - $\Rightarrow$ **Jet formation** & **Escaping accretion**
- accretor can be compact object, AGN

Two-component jet model

- **close to engine: GR mechanisms launch inner jet**

  $\Rightarrow$ efficient extraction AM from inner disk $+$ black hole (Blandford-Znajek mechanism)

  $\Rightarrow$ fast rotating inner jet, introduce **radially layered jet**

  $\Rightarrow$ inner $\Gamma \sim 30$, outer $\Gamma \sim 3$

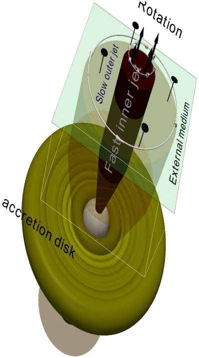

- perform 2.5D runs in cross-section
  - $\Rightarrow$ both HD and MHD runs
  - $\Rightarrow$ explore differences in effective inertia
- study jet integrity for axisymmetric runs
  - $\Rightarrow$ vary precise spine-sheath structure

Meliani & Keppens, ApJ 705, 1594-1606 (2009)

- vary relative contribution inner jet to total $L_{\mathrm{Jet,Kin}} \sim 10^{46} \mathrm{e}rgs/s$

  $\Rightarrow$ discover **new relativistic, centrifugal Rayleigh-Taylor**

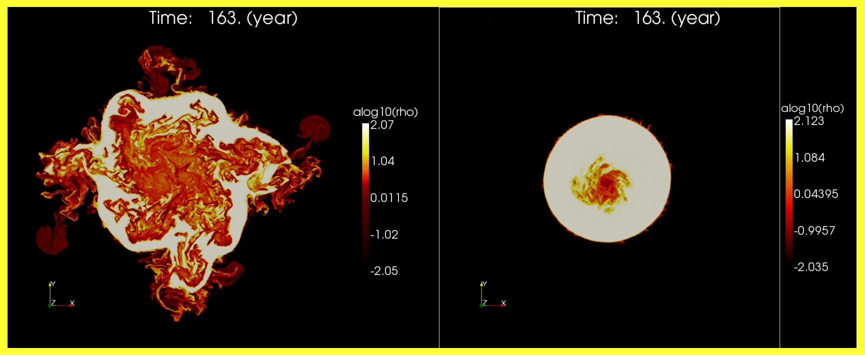

$\Rightarrow$

efficient AM redistribution, enhance inner/outer jet mixing

- novel **relativistically enhanced Rayleigh-Taylor mode**
  - $\Rightarrow$ **Stable: effective inertia outer $>$ inner jet**
  - $\Rightarrow$ **No classical counterpart** (relativistic flow essential)!
  - $\Rightarrow$ $\Gamma^2 h$ effect with h specific enthalpy
- stable versus unstable jets: **design initial conditions with varying contribution inner/outer jet to total kinetic energy**
  - $\Rightarrow$ criterion predicts cases A, C, D stable; B1, B2 unstable
  - $\Rightarrow$ **evolution of inner jet mean Lorentz factor**

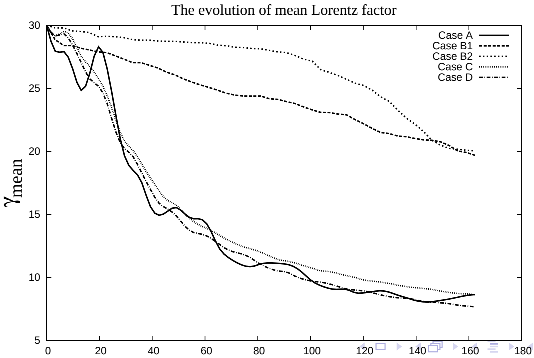

- novel **relativistically enhanced Rayleigh-Taylor mode**

  $\Rightarrow$ approximate **dispersion relation**

  $\Rightarrow$ insert spatio-temporal dependence $\exp(\lambda t - k \mid \zeta \mid)$ with displacement ζ

$$\lambda^2 \propto k \left[\left(\Gamma^2 \rho h + B_z^2 \right)_{\mathrm{in}} - \left(\Gamma^2 \rho h + B_z^2 \right)_{\mathrm{out}} \right]$$

- **Stability: effective inertia outer jet $>$ inner jet**

  $\Rightarrow$ works for both HD and MHD relativistic jets

  $\Rightarrow$ purely poloidal **B** effect incorporated

  $\Rightarrow$ **relativistic EOS crucial**: cold/hot outer/inner jet

- can quantify jet de-collimation due to mode development

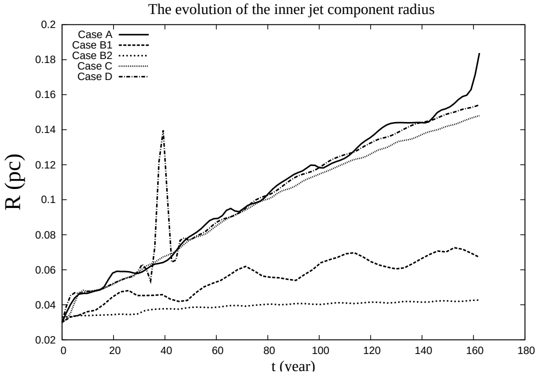

$\Rightarrow$ due to non-axisymmetric mode development

$\Rightarrow$ relativistic RT decelerates inner, decollimates total jet

- **FR II/FR I transition thereby related to central engine**

$\Rightarrow$ depends on distribution kinetic energy over two-component jet

Helically magnetized jets

- Axisymmetric **helical field configurations**
  - $\Rightarrow$ again 2.5D, density contrast $1/10$: light jet
  - $\Rightarrow$ inlet profile of Γ and $\mu = \frac{R_j B_\varphi}{R B_Z}$

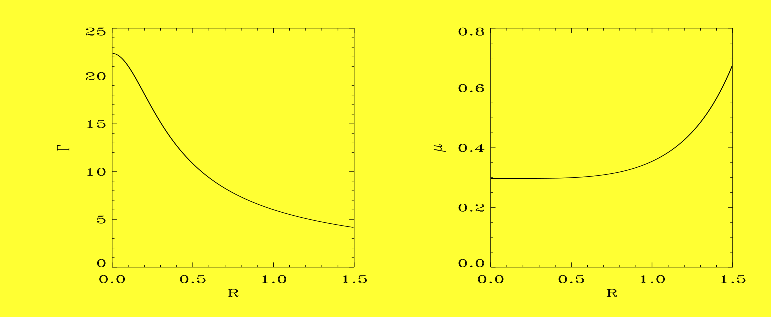

- average $\bar{\Gamma} \simeq 7$, $\beta_l = 0.3$ and $\sigma = 0.006$
  - $\Rightarrow$ **kinetic energy dominated, near equipartition**
- both helical field and rotation within jet!

- magnetic field: **helicity throughout the jet beam**
  - ⇒ changes at internal cross-shocks
  - ⇒ localized mainly toroidal field within vortical backflows

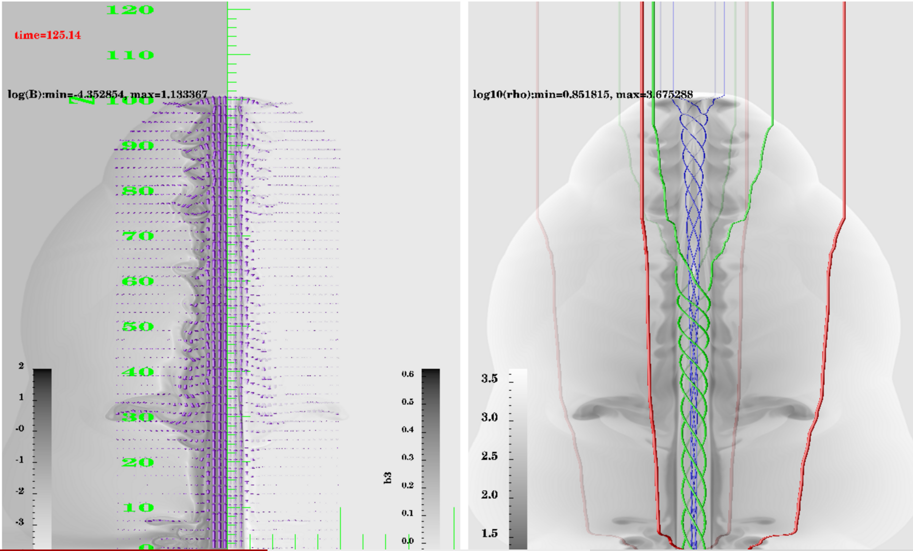

- beam cross-shocks: **helical field pinches flow**
  - $\Rightarrow$ matter reaccelerates up to next cross-shock
  - $\Rightarrow$ deceleration jet with equipartition $\mathbf{B}$: extreme lengths

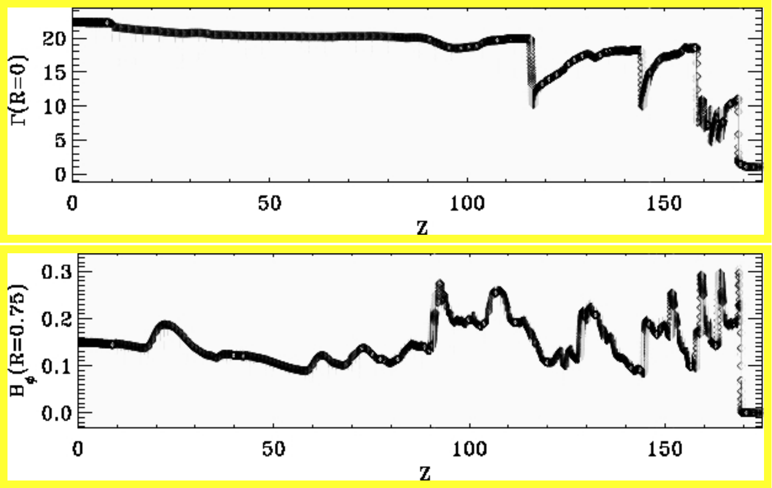

- detailed variation of field quantities at jet head
  - $\Rightarrow$ significant 2D effects compared to 1D Riemann problems

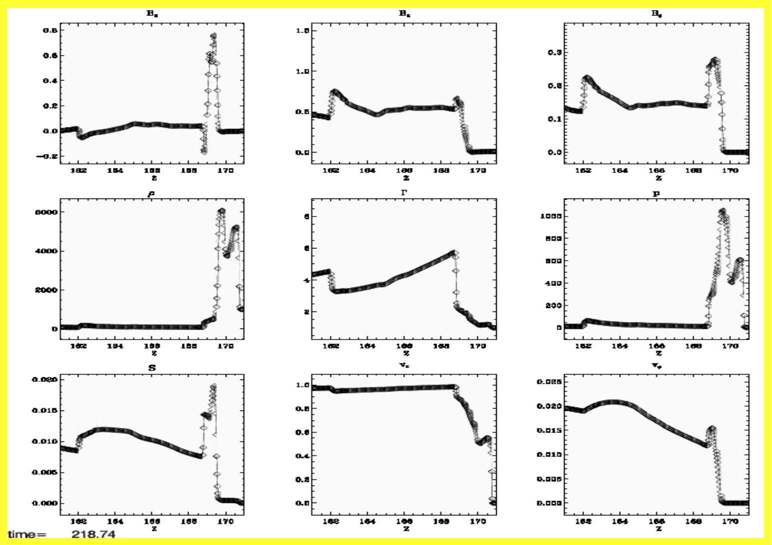

- quantified propagation characteristics

- explored transition $\bar{\Gamma} = 1.15 \rightarrow 7$

  $\Rightarrow$ non-relativistic: **strong toroidal field in cocoon**

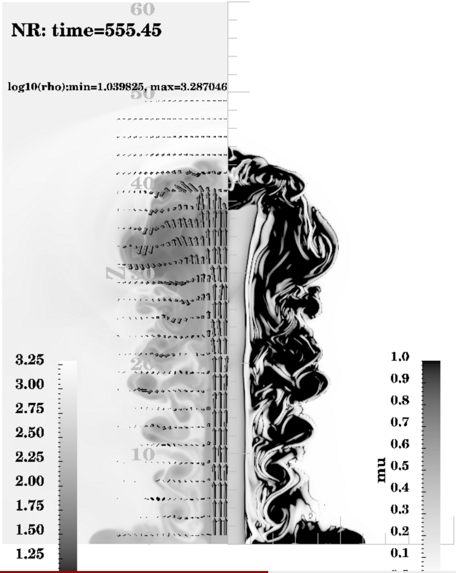

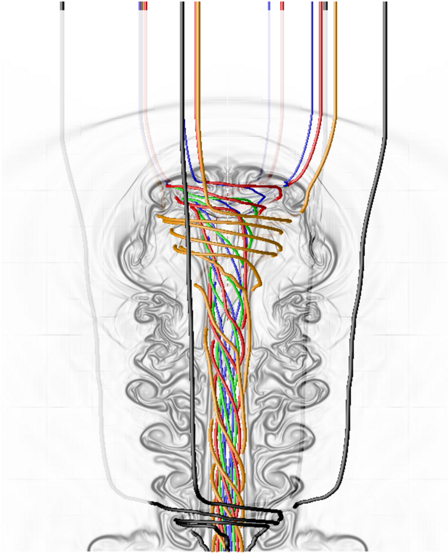

- power maps give **indication of sites of synchrotron emission**
  - $\Rightarrow$ total radiation emitted is $\propto v^2 \Gamma^2 B^2 \sin^2 \Psi$
  - $\Rightarrow$ varies significantly from toroidal to poloidal field cases
  - $\Rightarrow$ simultaneous plots of pressure/temperature at right

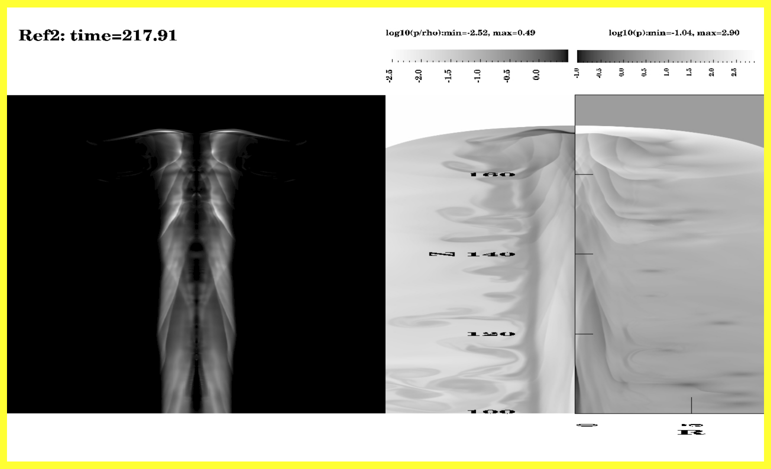

- Porth (2013): look at 3D MHD jet launch issues

  $\Rightarrow$ mimic keplerian disc corona, start from monopole-flared magnetic field

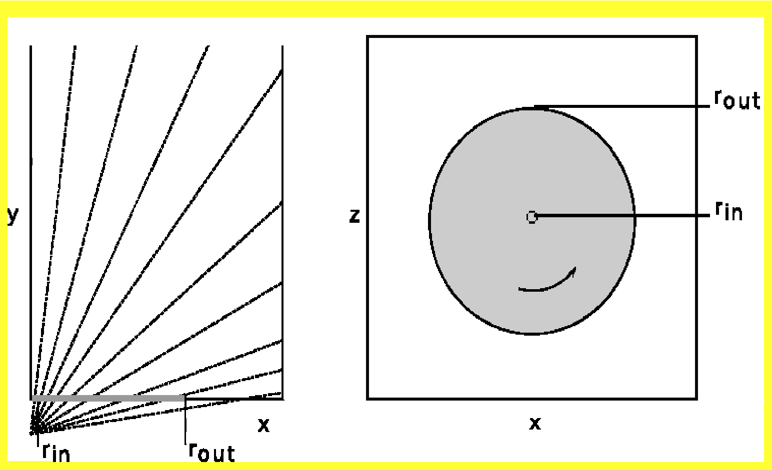

- jet self-collimates, reaches $\Gamma \simeq 2$ speeds

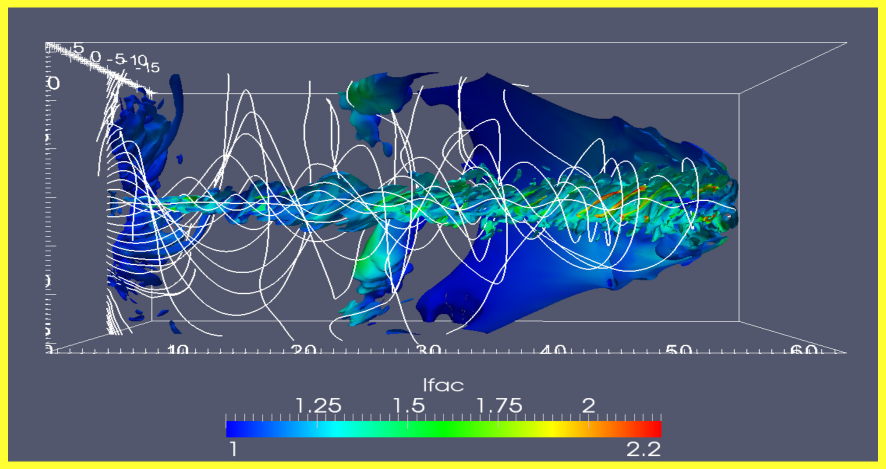

- quantify poloidal mode dominance along the jet

  $\Rightarrow$ barycenter location: axial deviations only beyond 70-80 disc radii: **self-stabilizes to kink**!

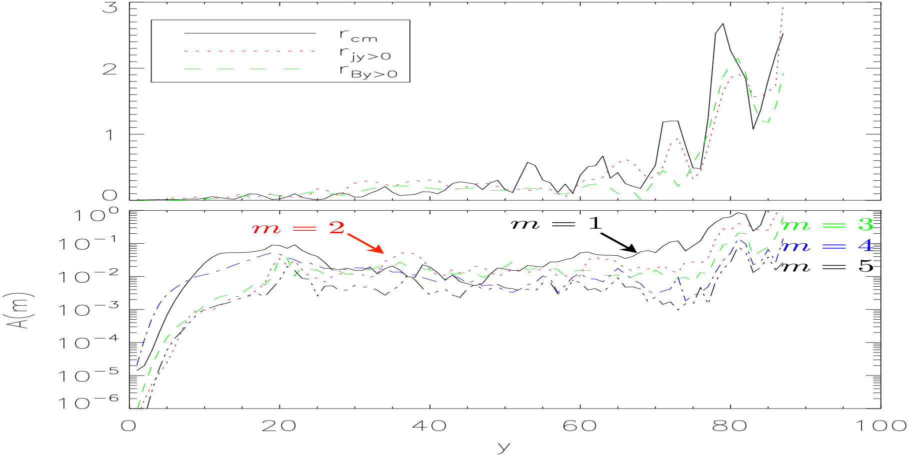

- pitch profile, and electric force (black) and Lorentz force (white)
  - $\Rightarrow$ electric forces counteract magnetic contribution!

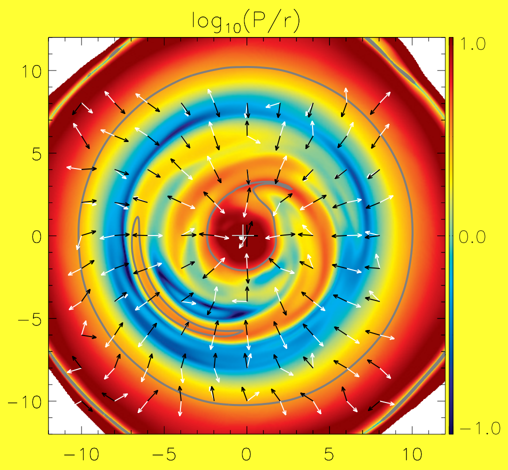

- to get significant non-axial perturbation: clumpy medium

  $\Rightarrow$ toroidal field has decreased: jet seeks path of least resistance, still kink-stable!

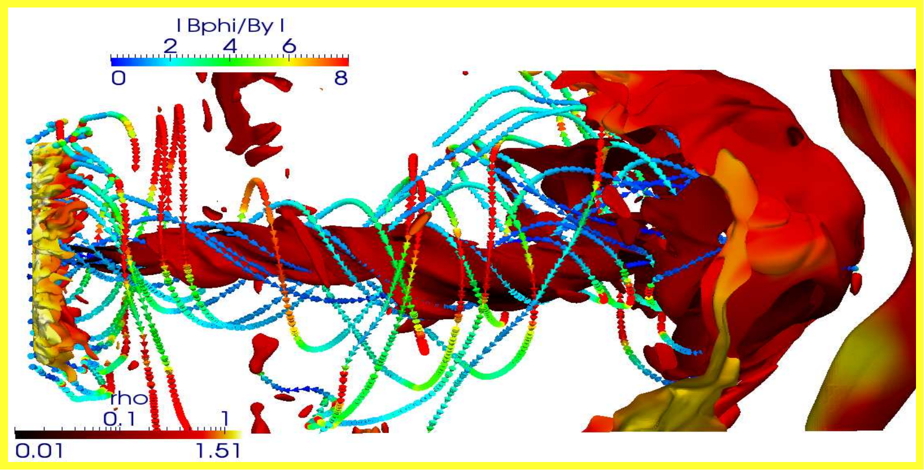

- filamentary current layer structure develops: particle acceleration sites & reconnection!

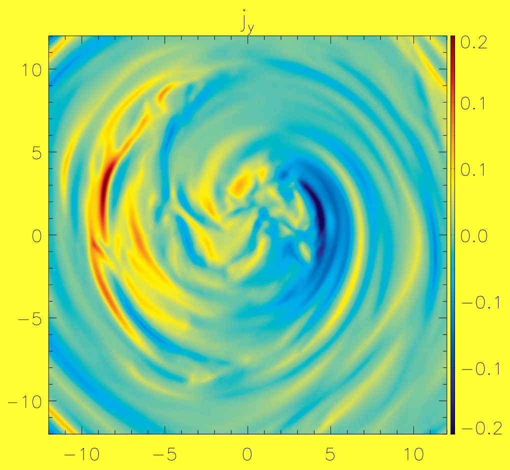

- *summary:* relativistic MHD models for AGN jets

  ⇒ radial stratification: mixing in 2-component (M)HD jets (spine-sheath) due to relativistic RT

  ⇒ helical **B**: magnetic reacceleration at cross-shocks

  ⇒ self-consistent stabilization to kink during launch from disc

- **Related References:**

  ⇒ Keppens & Meliani, Phys. of Plasmas 15, 102103, (2008)

  ⇒ Keppens et al., A&A 486, 663 (2008) **A&A Highlight**

  ⇒ Meliani & Keppens, ApJ 705, 1594 (2009)

  ⇒ Keppens et al., JCP 231, 718 (2012)

  ⇒ Porth, MNRAS 429, 2482 (2013)

Crab Pulsar Wind Nebula studies

- Crab Nebula: 10 lightyears across, located at 7000 lightyears

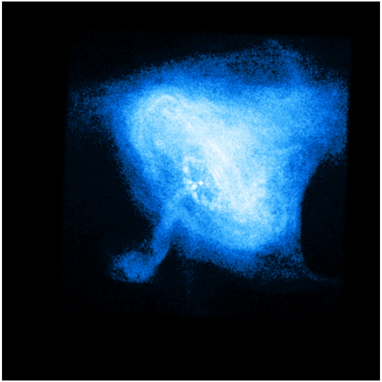

Astronomy picture of the day 2008 February 17, versus Chandra image, X-ray: smaller synchrotron nebula

- pulsar: rotating neutron star, remnant core of an exploded star
  ⇒ **pulsing in slow-motion** Lucky Imaging, Cambridge, 800 nm

  Period 33 msec: bright pulse, fainter interpulse: **lighthouse effect**
- X-ray light curve from ROSAT observations in 1991, one full cycle of 33 milliseconds

(Becker Aschenbach 94)

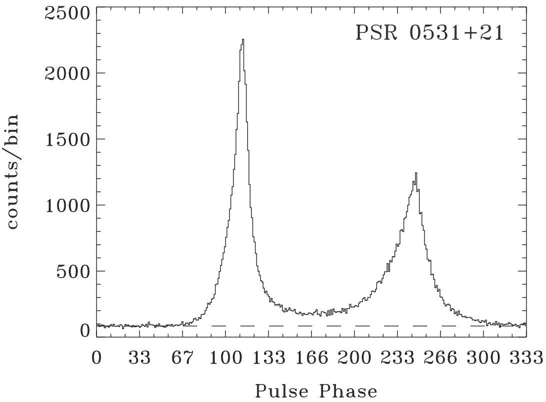

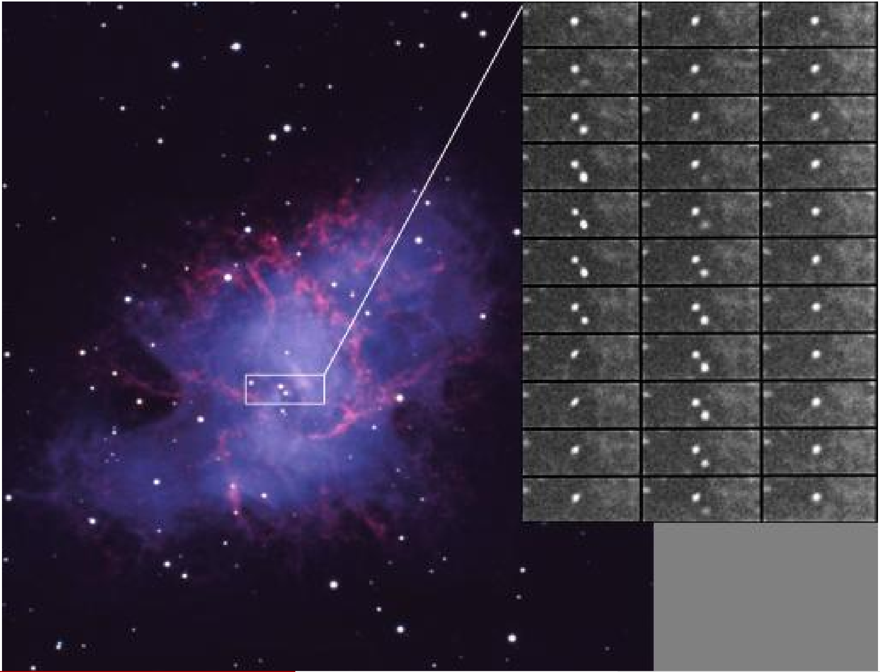

- environment shaped by rotating star $\approx$ 20 km across, $1.4 M_\odot$
  $\Rightarrow$ Becker & Aschenbach 1994: radius 7 – 16.1 km [various models take blackbody emission from neutron star surface, deduced surface temperature, varying EOS]

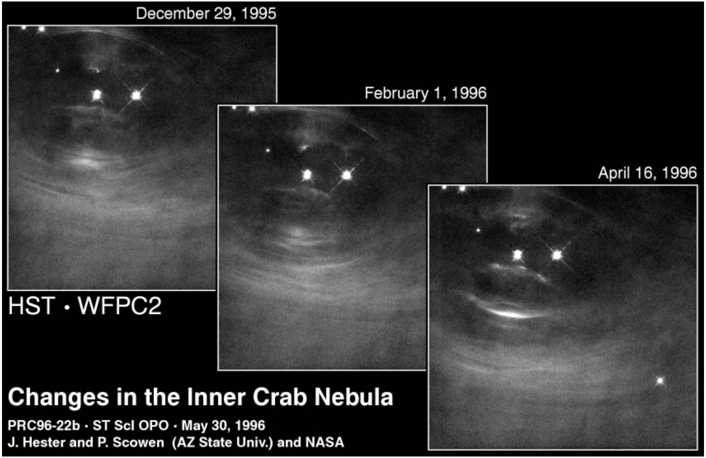

$\Rightarrow$ **ever closer up HST views** show wisps and 'sprite'

- pulsar has intense magnetic field, rotates 30 times per second
  - $\Rightarrow$ accelerates electrons, creating relativistic pulsar wind
  - $\Rightarrow$ pulsar+wind powers entire 10 lightyear-sized nebulae


(Hester et al, HST+Chandra, X-ray)

- **M1, with pulsar PSR 0531+21, is remnant of SN1054**
  - $\Rightarrow$ filamentary structure are the former stellar outer layers

- contemporary schematic of Crab nebula

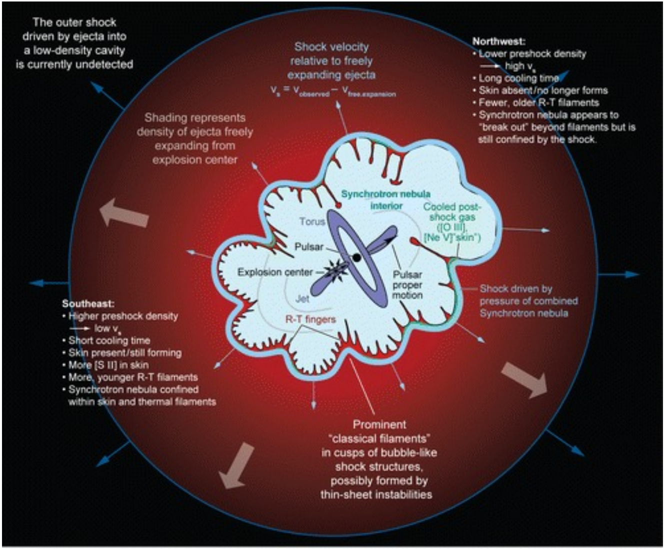

Hester JJ. 2008.
Annu. Rev. Astron. Astrophys. 46:127–55

- pulsar powers PWN (Pulsar Wind Nebula) which is confined and pushes into the freely expanding remnant [Hester 2008; Chevalier 1977]
  - $\Rightarrow$ PWN compresses ejecta into filamentary structure
  - $\Rightarrow$ PWN synchrotron radiation photoionizes ejecta
- synchrotron nebula outer boundary drives shock into freely expanding ejecta: itself bounded by an (unseen) shock marking expanding ejecta cloud

Synchrotron nebula

- pulsar spinning down: 'spin-down luminosity' $\sim 130000\ L_\odot$ (energy loss per second)
- kinetic energy dominated 'cold fast wind' surrounds pulsar proper, itself bounded by shock

  $\Rightarrow$ momentum balance (wind-nebula) quantifies shock position at 3×10^{17} cm (about 10^{11} pulsar radii!)

- synchrotron nebula = shocked pulsar wind zone

  $\Rightarrow$ hot plasma filling the synchrotron nebula is beyond the 'cold fast wind' shock location,
  shows quite some finestructure and dynamics

  $\Rightarrow$ roughly fills volume of $\approx 30\,\mathrm{pc}^3$

  $\Rightarrow$ very efficient into converting energy into synchrotron emission (up to 26% of injected energy)

  $\Rightarrow$ full energy content for nebula $\mathcal{O}(10^{49})$ ergs, translates to equipartition average magnetic field strength there of 300 μG

  $\Rightarrow$ most energy emitted from optical to X-ray

- HST (optical) and Chandra (X-ray) and VLA (radio) views combined show **wisps, sprite, jet, torus** all rather dynamic

  $\Rightarrow$ wisp width 1 arcsec, moves up to 0.5c

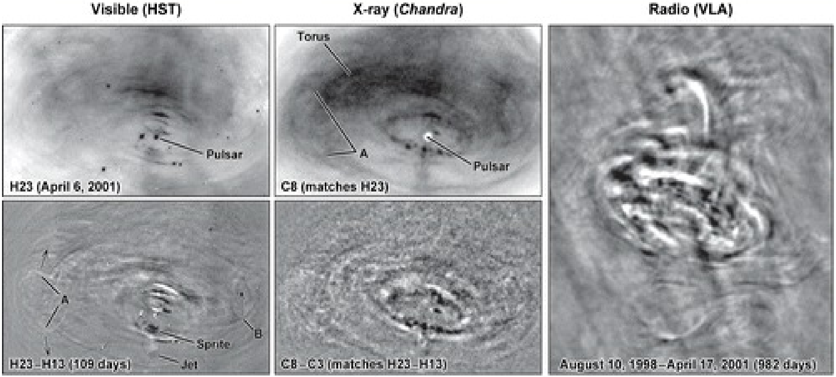

Hester JJ. 2008.
Annu. Rev. Astron. Astrophys. 46:127–55

$\Rightarrow$ inner ring (about a dozen knots in X-ray) and 'sprite' interpreted as quasi-stationary shock [Hester et al 2002]

$$\sigma = \frac{\text{EM energy (Poynting) flux}}{\text{kinetic energy flux}}$$

- PWN theory has a σ-problem:
  - $\Rightarrow$ pulsar magnetosphere and wind models say $\sigma \gg 1$
  - $\Rightarrow$ getting the right sizes in 1D PWN models requires $\sigma \ll 1$

Virtual views: the modeling part

- near-pulsar magnetosphere: extreme B up to 10^{12} G
  $\Rightarrow$ solve for EM fields, assume perfect conducting plasma, inertia negligible, about rotating perfectly conducting sphere
  $\Rightarrow$ 3D dipole B-field, misaligned magnetic-rotation axis (needed for pulse!) **force-free models Spitkovsky 2006**

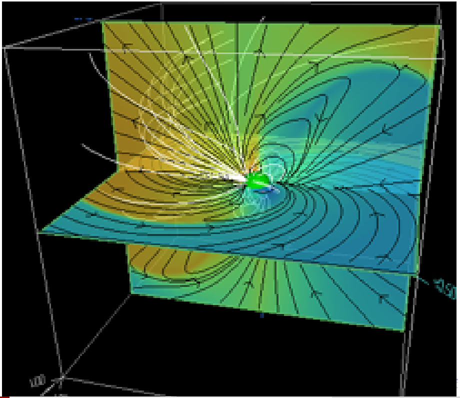

- **warped current sheet results!** seperates north-south hemisphere, beyond last closed fieldline

similar to heliospheric current sheet, ballerina skirt

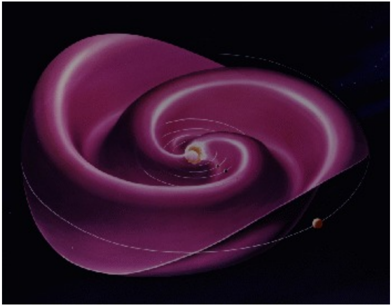

$\Rightarrow$ oblique rotator feeds magnetosphere EM energy (Poynting flux, high σ)

- allows to quantify spin-down as function of obliquity angle

- this fills entire pulsar wind zone: **striped wind**

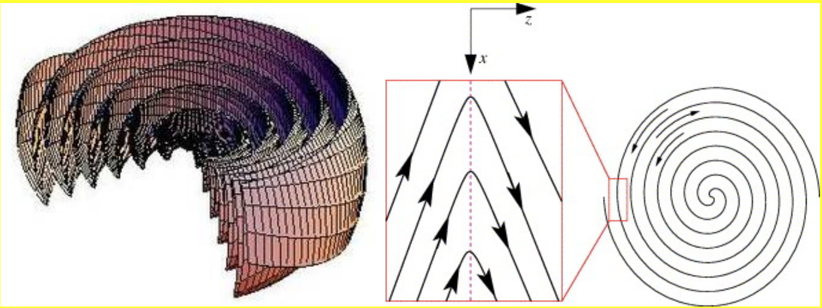

Kirk 2006

$\Rightarrow$ right top view: effective 'reconnection' throughout

$\Rightarrow$ converts EM to internal energy and lowers σ, but more is needed (e.g. no effect at poles)

σ-problem and the spherical cow ...

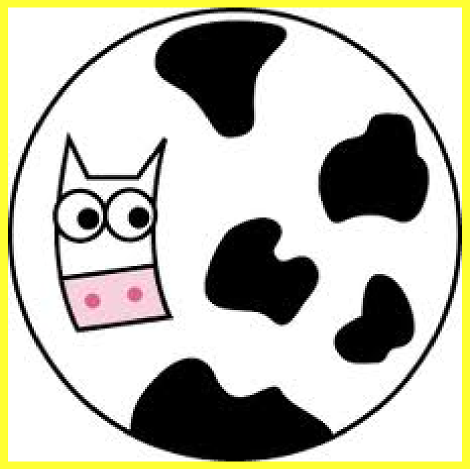

- Rees&Gunn 1974: wind zone ends at 3×10^{17} cm, at shock, while $\sigma \approx 0.01 - 0.1$ beyond this shock and throughout the PWN

- How reconcile wind zone has $\sigma > 1$ with low σ through PWN?
  - $\Rightarrow$ make a **cylindrical** cow:

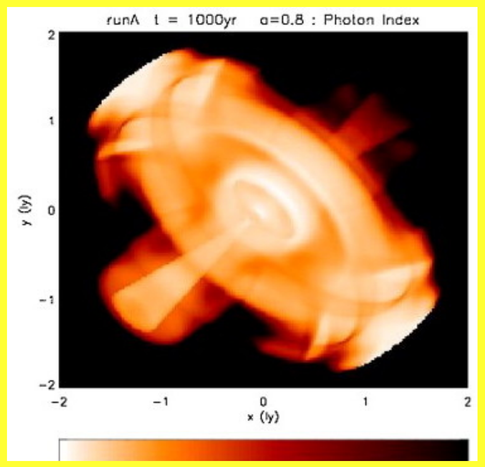

Bucciantini 2008

- perform relativistic MHD modeling: flat (Minkowski) space-time
  $\Rightarrow$ particle + energy-momentum conservation, full Maxwell equations, ideal MHD: vanishing electric field in comoving frame
  $\Rightarrow$ assume axisymmetry, solve shocked wind-PWN structure on 2D domain (Del Zanna et al. 2004)

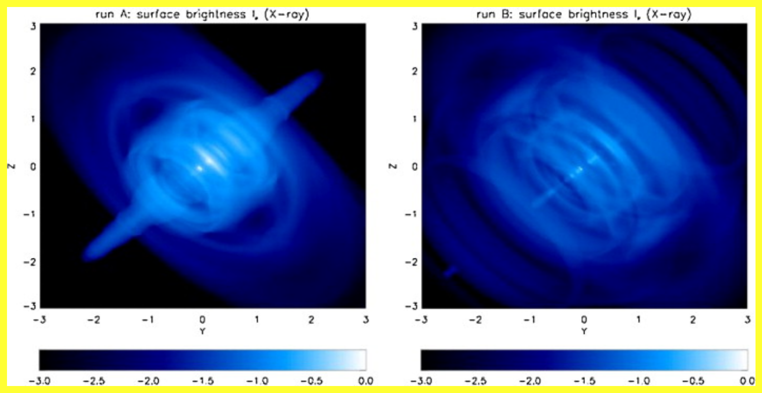

- 2.5D surprising agreement between models-observations
  - $\Rightarrow$ 1 knot; 2 wisps; 3: torus; 4: anvil; 5: bakside wisps

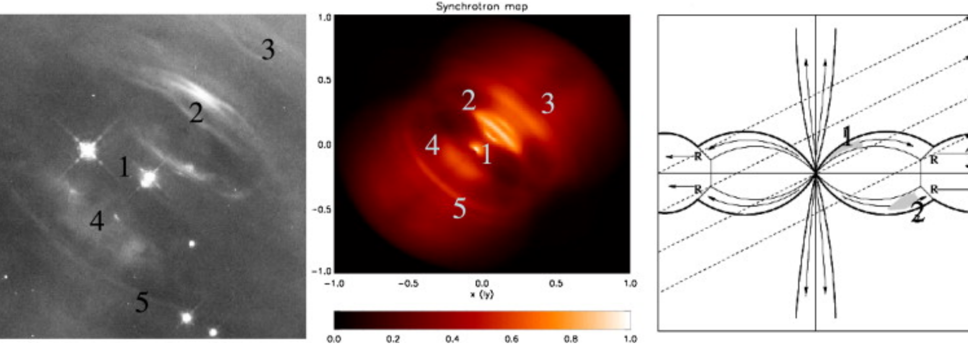

Hester 1995 & Komissarov-Lyubarski 2004 & Bucciantini 2008

But a real cow is 3D . . .

- **cross-sectional view: 3D versus 2.5D**

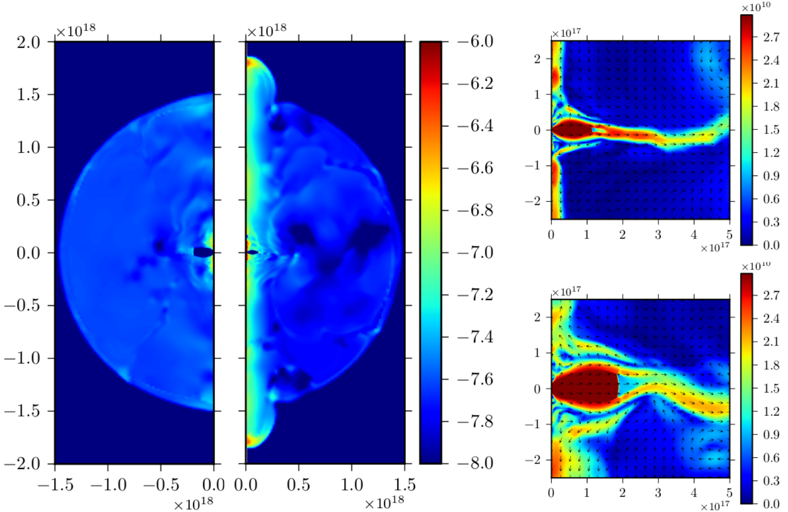

Porth et al. 2013

- initial setup: radially expanding supernova, surrounding unshocked pulsar wind

  $\Rightarrow$ pulsar wind prescription: captures high σ injection case, parametrized pole-to-pole variation of purely azimuthal field input due to striped wind, Lorentz factor 10 radial outflow

  $\Rightarrow$ first adjusts to self-consistently created free-wind to shocked wind nebula

  $\Rightarrow$ **shocked wind redirected in jet**

- 3D (special) relativistic MHD simulations (Porth et al 2013)
  - ⇒ strong toroidal field wind zone, termination shock
  - ⇒ poloidal field creation, significantly randomized field

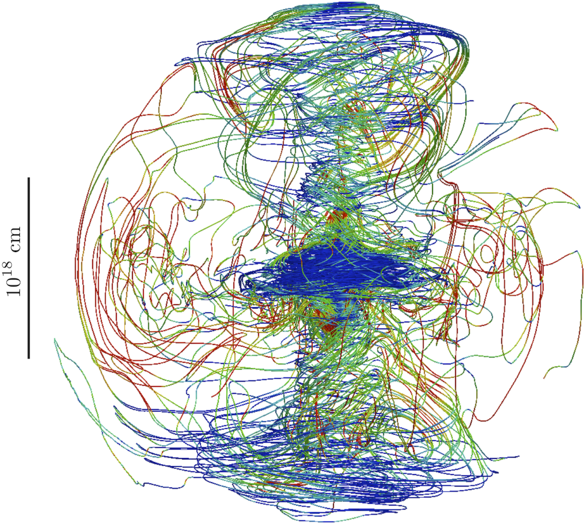

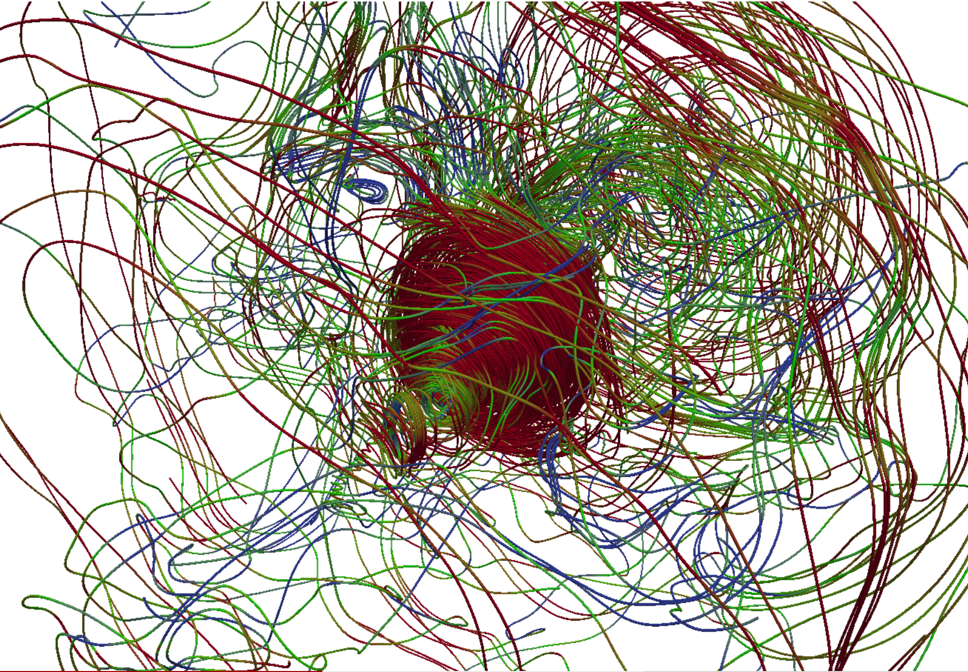

- **solved σ problem!**
  - $\Rightarrow$ size of wind region, shock distance as observed
  - $\Rightarrow$ striped wind prescription essential ingredient
  - $\Rightarrow$ 3D allows effective (kink instability) mixing (equator+pole)
  - $\Rightarrow$ PWN gas pressure dominated due to magnetic dissipation
  - $\Rightarrow$ synchrotron views: **vortex shedding as 'wisps'**

- **Observed X-ray + HST view**

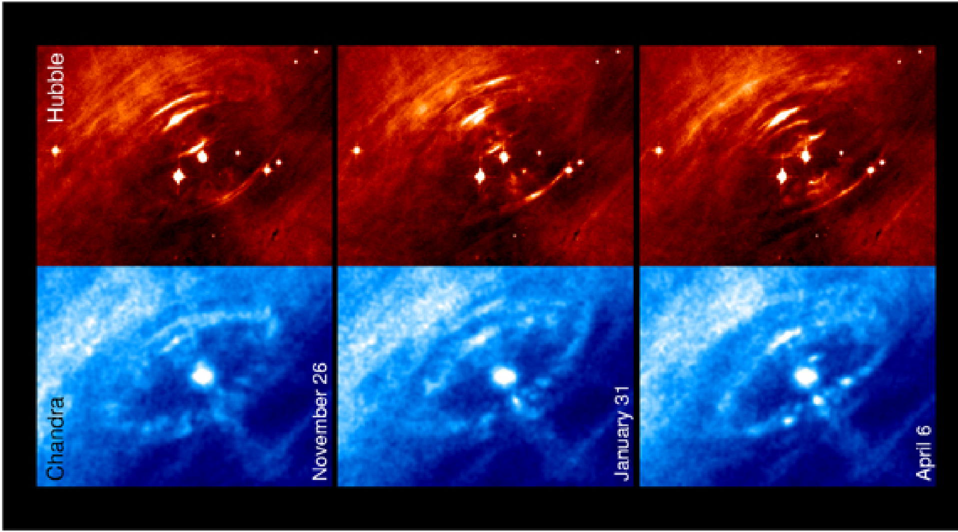

Simulated Chandra X-ray view

- composite image in X-ray, visible, radio


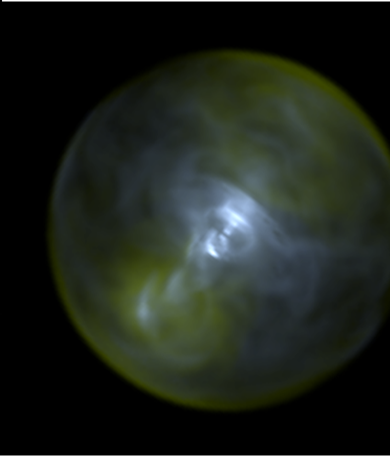

$\Rightarrow$ captures size difference in nebula extent at $\neq$ wavelengths

Outlook

- relativistic MHD: relax the $v \ll c$ assumption

  $\Rightarrow$ stressed special relativistic, ideal MHD

  $\Rightarrow$ modern efforts: GRMHD in evolving spacetimes, ideal to resistive RMHD, extremely energetic events (magnetars, GRB engines, ...)
- applications to relativistic jets (microquasar, AGN, GRB), PWN

  $\Rightarrow$ synthetic observations confront reality!
- future: cross-scale challenges (reconnection and microphysics, large scale collimated and accelerated flow patterns)